Battery State of Charge Estimation Using Guided Waves—Numerical Validation and Statistical Analysis

PURIM LADPLI, FOTIS KOPSAFTOPOULOS
and FU-KUO CHANG

ABSTRACT

This work presents a novel scalable and field deployable framework for estimating battery state of charge (SoC) based on pitch-catch guided wave propagation using low-profile built-in piezoelectric transducers. A preliminary study is performed through experiments using piezoelectric disc transducers mounted on commercial lithium-ion (Li-ion) pouch batteries. Similar experiments are carried out on Multifunctional Energy Storage (MES) Composites, which are an energy-storing structural material recently developed by the authors. In this work, special emphasis is given to the numerical validation of the variation in guided wave time of flight (ToF) due to the SoC-induced changes in electrode mechanical properties. The experimental results are accurately captured in the numerical simulation, which provides significant insight on the complex coupling between electrochemistry and mechanics. Moreover, a first-pass statistical analysis is conducted which demonstrates the efficacy of using guided wave data to obtain accurate prediction of battery SoC. The study also reveals a promising opportunity for exploiting the feature-rich multi-path nature of guided wave propagation to further improve SoC prediction accuracy.

INTRODUCTION

Extensive research effort in energy storage, particularly in lithium-ion (Li-ion) batteries, has been ongoing in response to the ever-growing demand for high-energy, light-weight energy solutions for portable devices, electric systems, and transportation [1, 2]. Yet, their broader practical adoption has been hindered by the system's reliability, lifespan, safety, and cost. The complexity of Li-ion batteries and their narrow operational envelope require accurate real-time state monitoring for effective control and management. Conventional on-board battery management systems (BMS) are currently limited to the monitoring of extrinsic parameters including voltage, current, and temperature [3, 4]. From these, battery state of charge (SoC) is merely approximated using state-estimation software and algorithms. The current techniques have not come

Purim Ladpli, Fotis Kopsaftopoulos, Fu-Kuo Chang, Department of Aeronautics and Astronautics, Stanford University, Stanford CA 94305, USA

to exploit the fact that a Li-ion battery fundamentally is a composite material system which undergoes mechanical evolution during electrical cycling. Thus, the mechano-electrochemical coupling presents an opportunity for guided wave techniques to be used for estimating SoC, similarly to how structural states are monitored in the context of structural health monitoring (SHM) [5].

To our best knowledge, there have been similar efforts attempting to use ultrasonic measurements for probing Li-ion batteries. In the study by Sood et al., only detrimental delamination of electrodes is detected through wave propagation, and SoC is not quantified [6]. Comprehensive studies by Gold et al. and Hsieh et al. show a trend of signal parameters on Li-ion cells during charging and discharging, but SoC is not quantified [7, 8]. Additionally, all previous studies are based on through-thickness transmitted and reflected bulk waves, which usually need external bulky ultrasonic probes and equipment, require extensive operator intervention, and suffer from inaccurate baseline collection.

Trying to address the aforementioned challenges, we introduce a scalable and field-deployable technique for battery SoC monitoring with ultrasonic guided waves, using minimal-footprint piezoelectric wafer transducers (Figure 1). Our previous work has shown promising results by experimentally demonstrating the correlation between guided wave signals and battery SoC and aging, and its applicability to battery monitoring [9, 10]. A continuation of the work is presented in this paper where special emphasis is given to the numerical validation of the SoC-induced change in guided wave signals, as well as the statistical analysis and predictive modelling.

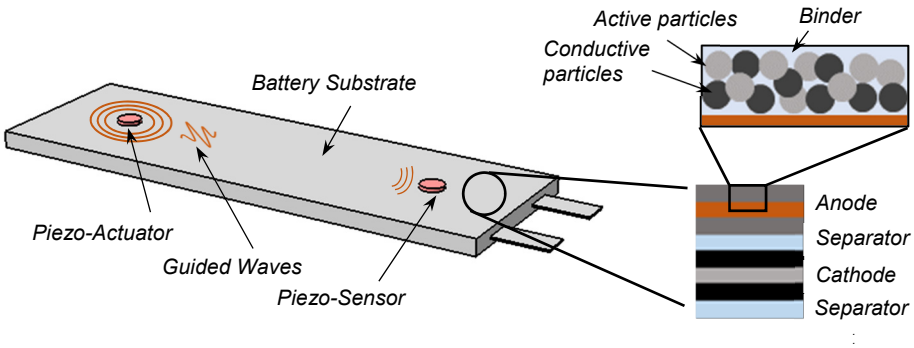

Figure 1. Schematics of ultrasonic guided-wave propagation in Li-ion battery substrate, using surface-mounted low-profile piezoelectric transducers.

Problem Statement and Method of Approach

SoC prediction is a challenging task for battery monitoring and management because on-field applications are often limited to rudimentary voltage measurements and computationally expensive prediction algorithms. In the previous companion work, we have demonstrated the correlation between experimental pitch-catch guided wave signals and battery SoC, as well as its applicability to SoC prediction [9, 10]. An actual implementation of the technique however requires a full understanding of the underlying physical relationship between electrochemistry and mechanics in order to establish a robust predictive modelling approach. Hence, it is imperative to thoroughly

investigate the intertwined coupling between the electrochemical process and the mechanical wave propagation. Then, a statistical framework needs to be developed to analyze and fully utilize the feature-rich multi-path nature of guided wave signals for SoC prediction.

Therefore, this work places special emphasis on the numerical validation of the variation in guided wave time of flight (ToF) as a function of battery SoC. The experimental ToF is compared with the results from a numerical simulation using gathered geometry data and values of electrode moduli and densities. In addition, a preliminary statistical analysis is performed on the experimental data to evaluate the overall SoC prediction accuracy using guided waves. We then explore different model structures to evaluate the efficacy of improving the prediction accuracy by using multiple extracted signal features from multiple propagation paths.

PRELIMINARY EXPERIMENTAL RESULTS

The experimental setup and preliminary results, which the numerical validation and statistical analysis are based on, have been discussed in our previous companion work, but for the sake of completeness they will be repeated herein [9, 10]. In brief, pitch-catch guided wave propagation experiments are performed on 3,650mAh off-the-shelf Li-ion pouch batteries, as well as on 4,000mAh MES Composite cells, which are a new type of structurally reinforced Li-ion battery recently developed by the authors [10-13]. Guided wave signals are gathered at various battery SoCs from four surface-mounted piezoelectric disc transducers (6.35mm-diameter PZT-5A in the SMART Layer format (Acellent Technologies, Inc.) at the locations shown in Figure 2. The pitch-catch experiments use standard five-peak Hanning-windowed tone bursts with center frequencies between 100 to 200 kHz. A total of four propagation paths are under study, i.e. Path 1 from transducer P1 to P3, Path 2 from P1 to P4, Path 3 from P2 to P3, and Path 4 from P2 to P4. The ultrasonic data acquisition is synchronized with a battery cycler which performs battery charging and discharging, allowing SoC to vary from 0% at a fully discharged state to 100% at a fully charged state.

In this work, only the time-domain analysis of the signals is discussed. A representative time-domain actuator-sensor response is shown in Figure 3 from a pouch cell experiment at a given SoC. Two time-domain parameters are of interest: the (sensing) signal amplitude, which is the maximum amplitude of the sensing signal's Hilbert envelope, and the time of flight (ToF), which is the measure of the time taken by an actuation wave packet to reach a sensor. The change in battery SoC results in the behavior of the time-domain signal parameters shown in Figure 3b for a representative pouch cell and in Figure 3c for an MES Composite cell. This mechano-electrochemical correlation is numerically validated and statistically analyzed in the subsequent sections.

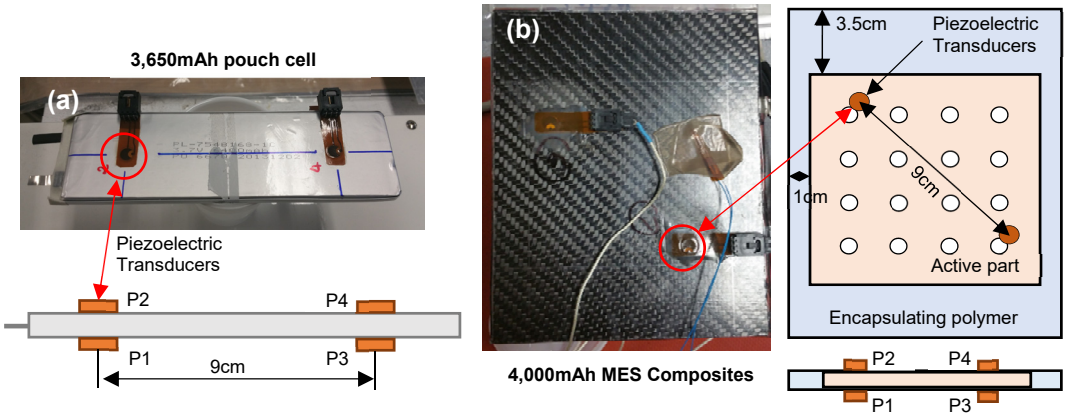

Figure 2. Locations of the four surface-mounted piezoelectric transducers labeled P1 through P4 on (a) a 3,650mAh Li-ion pouch cell and (b) a 4,000mAh MES Composite battery.

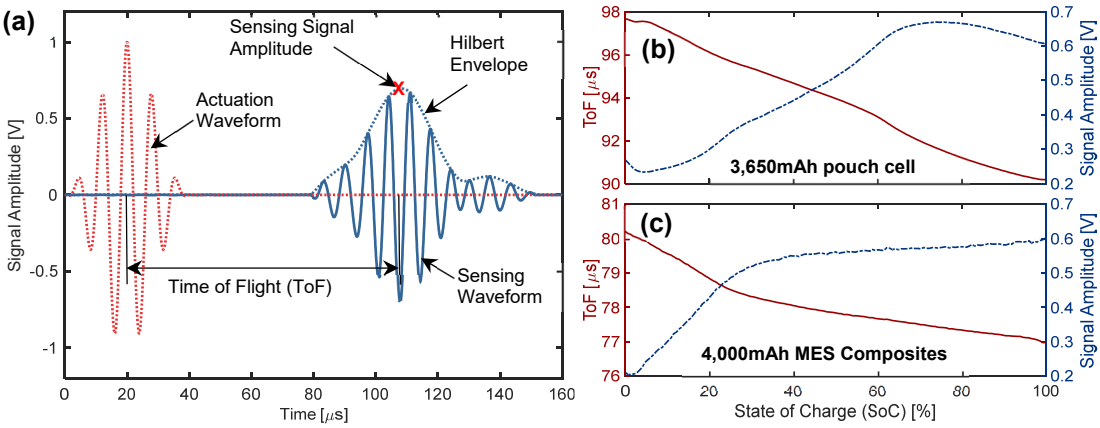

Figure 3. (a) Representative signals from the P1-P3 transducer pair at 125 kHz, showing the definition of time of flight (ToF) and signal amplitude; (b) evolution of ToF and signal amplitude with respect to the change in SoC observed in a representative pouch cell (Path 1 (P1-P3) at 125kHz); (c) ToF and signal amplitude from Path 1 at 125 on an MES Composite cell.

NUMERICAL VALIDATION OF TIME OF FLIGHT VARIATION

Li-ion batteries are fundamentally a composite material system that undergoes mechanical and chemical changes as they cycle. As a battery undergoes charging and discharging, the moduli and densities of the constituent electrode materials change. The intertwined electrochemical coupling of the composite anode and cathode, as well as the complex acoustoelastic physics in such an anisotropic interspersed medium, require a thorough wave propagation analysis to obtain accurate validation of the actual phenomenon, which will be described herein.

Modelling Method

The wave propagation in a Li-ion battery is investigated analytically using fundamental acoustoelastic principles in order to explore the effects of density and modulus on the guided wave ToF. The dispersion characteristics of the wave

propagation in a Li-ion multilayered structure is then solved numerically using the DISPERSE software [14, 15]. The wave velocity as a function of battery SoC can be obtained, from which ToF can be back-calculated. In this work, only the experimental results from pouch cells are validated due to the limitation of the software in allowing the three-dimensional presence of the rivets to be included in the case of the MES Composites.

To initialize the calculation, a functional relationship between SoC and electrodes' moduli and densities need to be established. The density and modulus values of all the constituent materials are gathered from published resources and are summarized in TABLE I. A Li-ion pouch battery is essentially a laminate of active electrode layers – i.e. anode and cathode, stacked in an alternating fashion with each adjacent layer separated by a thin porous polymer separator membrane. The anode and cathode themselves are also laminated materials comprising a thin metallic current collector foil (copper and aluminum for anode and cathode respectively) with an active electrode film coating on both sides. The last stage of anisotropy is in the active electrode film which is a homogeneous mixture of active microparticles (graphite for anode and nickel-manganese-cobalt-oxide for cathode) and electrically conductive particles, adhered together with a polymeric binder.

In TABLE I, the only parts which are functionally dependent on SoC are the active electrode films (both anode and cathode). The volume-weighted average values of density and modulus of the electrode films are then calculated and shown in Figure 4a. The modulus and density values of all the individual layers and their corresponding layer thickness are used as input data in DISPERSE. The group velocity and propagation time of flight are then obtained through the simulation of the laminate material system.

TABLE I. MECHANICAL PROPERTIES, LAYER THICKNESS AND VOLUME FRACTION OF CONSTITUENT MATERIALS IN THE 3,650MAH POUCH BATTERY. [16-19]

Components	Thickness [μm]	Constituent materials	Vol. frac. of constituent materials [%]*	Modulus [GPa]	Density [kg/m^3]	Ref.
Anode film	96	Active (graphite)	55	19.2-101.5	2.05-2.26	[16]
		Conductive particles	0	25	1.95	[17]
		Binder	5	2	1.77	[17]
Copper foil	10			100	8	
Cathode film	60	Active (metal oxide)	50.8	108.5-252.1	4.93-5.01	[18,19]
		Conductive particles	8.5	25	1.95	[17]
		Binder	4.7	2	1.77	[17]
Aluminum foil	10			70	2.7	
Separator	25			0.7	0.55	[17]

*The remaining volume in the active components is filled with organic electrolyte.

NOTE: The layer thicknesses and volume fractions are measured values

Results and Discussion

Figure 4b shows a comparison between the results from the DISPERSE simulation and the experimental ToF of signals from Path 1 (From transducer P1 to P2) at 125 kHz from an indicative pouch cell. A very good comparison agreement can be seen at higher SoC levels, but overall, the simulation accurately captures the decrease in ToF and the

curvature of the trend. The absolute change in ToF between the fully charged and discharged states is also captured reasonably well – approximately 8µs and 11µs for the experiment and simulation results respectively.

Because wave propagation velocity is approximately proportional to the square root of the modulus to density ratio, the decrease in ToF at higher SoC (faster propagation speed) is to be expected from the changes in the modulus and density values shown in Figure 4a. Despite the counter-intuitive decrease in the cathode modulus, it appears that the aggregate modulus-to-density ratio of the composite still increases as a result from the other three factors, which cause the wave to globally speed up.

Moreover, there are local non-linearities observed in the experimental ToF which cannot be accurately captured in the simulation. These non-linearities are primarily induced by the intercalation staging in the graphitic anode, and potentially in part to the concentration-limited phases of the cathode. The detailed transitioning of mechanical properties is not well documented in literature, but such characterization is currently under our investigation and will be included in a future paper. The interpretation of signal attenuation's behavior is also underway, even though numerical modeling of wave attenuation is not a straightforward task since the propagation involves anisotropy, porosity, interfaces, and multiple material phases. A full understanding of the underlying physical phenomena will become crucial when this concept is extended to battery aging and remaining life prediction because these mechano-electrochemical fingerprints can help pin point the root cause of battery failure.

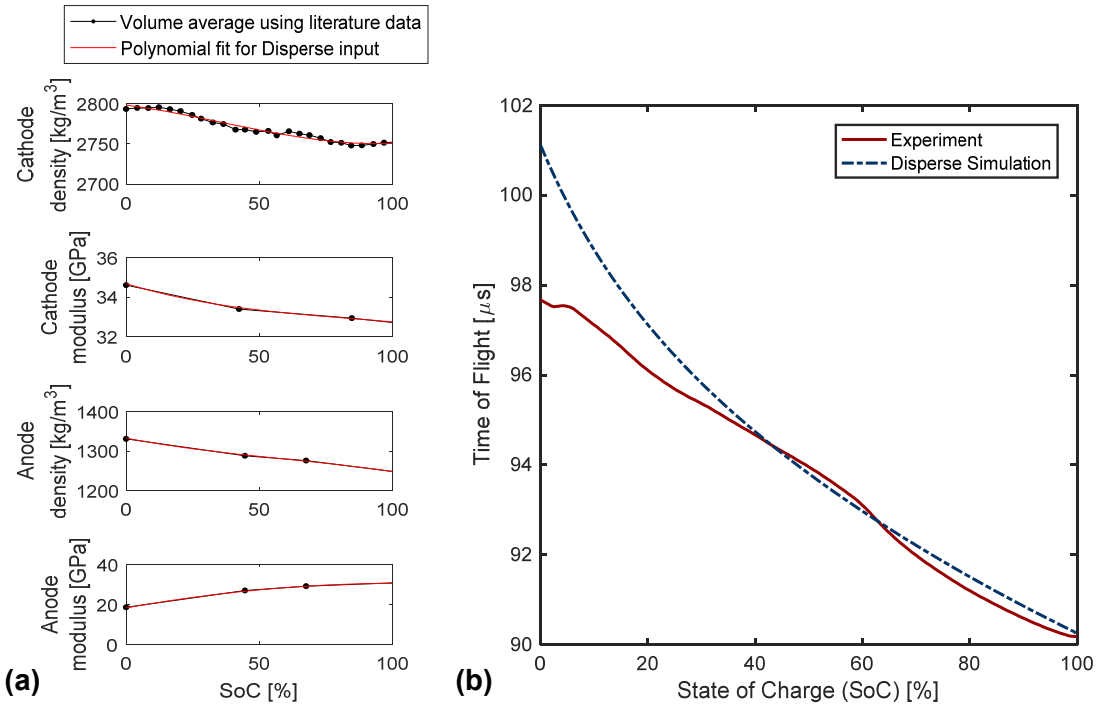

Figure 4. (a) Anode's and cathode's modulus and density variation with respect to the change in SoC calculated using volume-weighted average; (b) comparison between experimental ToF and numerical results from DISPERSE for signal from a pouch cell from Path 1 (P1-P3) at 125 kHz.

STATISTICAL ANALYSIS AND SOC PREDICTION

As previously discussed, conventional on-board BMSs rely mainly on current- and temperature-compensated voltage measurement to determine battery SoC. As a result, a lapse in measurement of this scalar value may potentially lead to inaccurate SoC prediction. This part of the work aims at exploring the concept of exploiting the multi-path, feature-rich nature of guided wave signals to attain better real-time SoC estimation. Therefore, we conduct a very fundamental statistical analysis and validate the feasibility of:

(i) improving the prediction accuracy by simultaneously using two ultrasonic features: ToF and signal amplitude
(ii) further reducing prediction error by using information from multiple paths
(iii) reducing the prediction model order without losing accuracy by maintaining data richness.

Statistical Method

A basic statistical analysis is performed by creating prediction models based on a Generalized Additive Model (GAM) [20]. GAMs are a non-parametric regression technique, which allows dependent variables to be described by smooth non-linear functions of covariates. GAMs with a Gaussian error distribution and identical link function are fitted on the data set from pouch cells and MES Composite cells to estimate SoC. Thin-plate regression splines are employed as smoothed fits of covariates using maximum penalized likelihood [21]. For each GAM, different sets of covariates are considered:

- **Model 1**: the only covariate is the ToF from Path 1 (P1 to P3) at 125kHz. (1 predictor)
- **Model 2**: the only covariate is the signal amplitude from Path 1 at 125kHz. (1 predictor)
- **Model 3**: ToF and signal amplitude from Path 1 at 125kHz are the covariates. (2 predictors)
- **Model 4**: ToF and signal amplitude from Paths 1 through 4 at 125kHz are the covariates. (8 predictors)
- **Model 5**: the same covariates as Model 4, but the maximum degree of freedom (d.f.) of each smoothed fit is limited to 2. (8 predictors, limited d.f.)

The above five model structures are then statistically compared to validate the use of multiple features and paths. The deviance explained, adjusted R^2, and generalized cross-validation (GCV), as well as 10-fold cross validation (CV) error and Akaike Information Criterion (AIC) [22] are calculated and compared for each of the models.

Results and Discussion

The GAMs and their statistical values are presented in TABLE II and TABLE III for data from a representative pouch cell and MES Composite cell respectively. The shapes of the functional forms of the covariates in the pouch cell Model 4 are illustrated in Figure 5 to indicate the non-linear relationship between SoC and the covariates. To elaborate on the first aim (improving the prediction accuracy by simultaneously using two ultrasonic features – ToF and signal amplitude), we first evaluate the statistical

results from Models 1 through 3. Using both ToF and signal amplitude as predictors, Model 3 shows lower AIC, GCV score, and 10-fold CV error than Models 1 and 2. This is true for all other signal paths, which are not shown here for the sake of abbreviation. Therefore, this confirms the feasibility of exploiting the feature-rich nature of guided wave data for SoC prediction accuracy improvement. However, a comparison between Models 1 and 2 indicates that ToF appears to be a better predictor of SoC than signal amplitude. This is to be expected due to the higher noise level and the abrupt changes in the curvature in the signal amplitude versus SoC plot (Figure 3). Feature extraction and selection thus become very crucial and care should be taken when constructing a prediction model using multiple signal features.

Model 3 can be further compared to Model 4 to investigate the added benefits of using an ensemble of data from multiple paths. With ToF and signal amplitude data from four distinct propagation paths, Model 4 exhibits significantly better prediction accuracy. All but one predictors in Model 4 are statistically significant (p-value < 0.001) and thus contribute to the SoC prediction accuracy improvement. The very low GCV score and 10-fold CV error (< 0.1 %SoC) from Model 4 also confirms that guided waves can be used to predict battery SoC to a very high accuracy.

Model 5 keeps the same predictors as Model 4 (8 predictors – ToF and signal amplitude from all four paths), but the maximum d.f. of each functional relationship is limited to 2. The prediction of accuracy of Model 5 is similar to that of Model 3 which uses two predictors without any limitation on the d.f. However, the structure of Model 5 involves much fewer d.f. than Model 3. This presents an opportunity for reducing the prediction model order by exploiting the multi-dimensionality of guided wave data, allowing good prediction accuracy to be achieved with low computational cost.

TABLE II. STATISTICAL RESULTS OF THE DIFFERENT SOC PREDICTION MODELS FOR DATA FROM A REPRESENTATIVE 3,650MAH POUCH CELL.

Parameters	**Model 1**		**Model 2**		**Model 3**		**Model 4**		**Model 5**	
Adjusted R^2	0.999		0.991		1		1		1	
Deviance explained (%)	99.9		99.1		100		100		100	
GCV score	0.947		7.87		0.265		0.057		0.331	
AIC	1647		2899		895		-19		1026	
global d.f.	10.9		10.6		19.2		43.6		9.57	
10-fold CV error	1.01		7.87		0.45		0.09		0.44	
	d.f.	**p-value**	**d.f.**	**p-value**	**d.f.**	**p-value**	**d.f.**	**p-value**	**d.f.**	**p-value**
Covariates										
Path 1 ToF	8.92	<0.001	-	-	9	<0.001	6.78	<0.001	1.84	<0.001
Path 1 Amplitude	-	-	8.56	<0.001	8.16	<0.001	0.13	0.323	0.38	<0.001
Path 2 ToF	-	-	-	-	-	-	7.28	<0.001	1	<0.001
Path 2 Amplitude	-	-	-	-	-	-	6.96	<0.001	1.46	<0.001
Path 3 ToF	-	-	-	-	-	-	6.51	<0.001	0.54	<0.01
Path 3 Amplitude	-	-	-	-	-	-	7.45	<0.001	1	<0.001
Path 4 ToF	-	-	-	-	-	-	3.12	<0.001	0.99	<0.001
Path 4 Amplitude	-	-	-	-	-	-	3.4	<0.001	0.37	<0.001

Approximate significance levels (p-value) and degrees of freedom (d.f.) are displayed for each of the covariates.

All in all, we have presented a first-pass statistical analysis of guided wave data with an attempt to explore the multi-feature, multi-path nature of guided wave signals for battery SoC prediction. It is important to note that this analysis is model-agnostic and is merely used to emphasize the benefits of this method over the scalar voltage measurement in a traditional BMS. There is room for improvement both in terms of the statistical modelling and the actual wave propagation implementation themselves. Nevertheless, it is shown that guided waves can be applied in conjunction with voltage-based prediction to further improve the estimation robustness and accuracy.

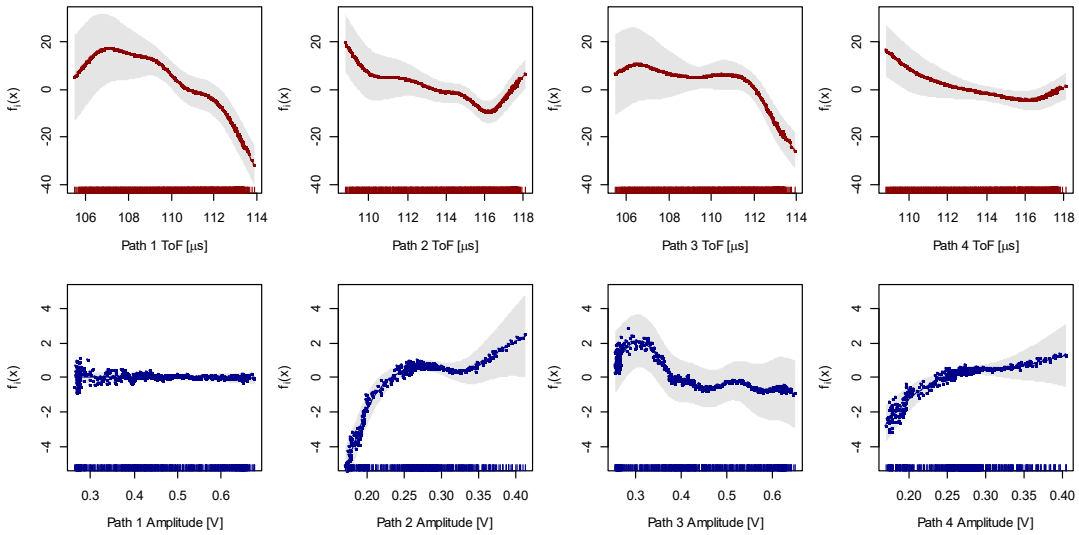

Figure 5. Example of the GAM components (spline functions) that constitute Model 4 in TABLE II. The tick marks on the x-axis are observed data points. Grey ribbons indicate 95% confidence bounds.

TABLE III. STATISTICAL RESULTS OF THE DIFFERENT SOC PREDICTION MODELS FOR DATA FROM A REPRESENTATIVE MES COMPOSITE CELL.

Parameters	**Model 1**		**Model 2**		**Model 3**		**Model 4**		**Model 5**	
Adjusted R^2	1		0.71		1		1		1	
Deviance explained (%)	100		72.5		100		100		100	
GCV score	0.398		261.98		0.35		0.057		0.29	
AIC	287		1254		266		-83		240	
global d.f.	10.5		9.7		18		46.8		7	
10-fold CV error	0.44		251.1		0.39		0.07		0.4	
	d.f.	**p-value**	**d.f.**	**p-value**	**d.f.**	**p-value**	**d.f.**	**p-value**	**d.f.**	**p-value**
Covariates										
Path 1 ToF	8.47	<0.001	-	-	8.88	<0.001	4.86	<0.001	0.42	<0.001
Path 1 Amplitude	-	-	7.66	<0.001	7.16	<0.001	6.67	<0.001	1.23	<0.001
Path 2 ToF	-	-	-	-	-	-	8.63	<0.001	1.59	<0.001
Path 2 Amplitude	-	-	-	-	-	-	0.86	<0.001	0	<0.001
Path 3 ToF	-	-	-	-	-	-	4.86	<0.001	0	<0.001
Path 3 Amplitude	-	-	-	-	-	-	7.33	<0.001	0.44	<0.001
Path 4 ToF	-	-	-	-	-	-	3.91	0.056	0.42	<0.001
Path 4 Amplitude	-	-	-	-	-	-	7.69	<0.001	0.92	<0.001

Approximate significance levels (p-value) and degrees of freedom (d.f.) are displayed for each of the covariates.

CONCLUSIONS

In summary, this work established a preliminary evaluation of battery SoC prediction using ultrasonic guided waves with surface-mounted piezoelectric transducers on commercial Li-ion pouch batteries and MES Composite cells. Special emphasis was given to the numerical validation of the SoC-induced variation in ToF and a first-pass statistical analysis of SoC prediction using guided wave data. In essence, it has been shown through our study that:

- The changes in moduli and densities of Li-ion battery electrodes at various SoCs affect the guided wave propagation within the battery medium. Numerical modelling of the ToF signature using the DISPERSE software shows a good agreement with the experimental results, setting the stage for detailed wave propagation analysis.
- A preliminary statistical analysis has shown that SoC can be predicted using guided wave data with high accuracy. Moreover, we have shown the potential of exploiting the feature-rich, multi-path nature of guided wave signals to enhance prediction accuracy and reduce prediction model order.

Further detailed analysis is underway for the correlation of the guided wave signal attenuation with the battery physical phenomena at different SoCs, as well as the investigation and modelling of the local non-linearities. Last but not least, the preliminary statistical study presented heretofore will be used in the development of a robust and accurate prediction model that employs smart feature extraction and selection, and compensation for operating conditions and environments.

ACKNOWLEDGEMENTS

The work is supported by the Advanced Research Projects Agency - Energy (U.S. Department of Energy) through the ARPA-E Award No. DE-AR0000393. The authors greatly appreciate support from Dr. Keith Kepler, Dr. Hongjian Liu, and Dr. Michael Slater at Farasis Energy Inc. for valuable feedback and suggestions.

REFERENCES

1. Goodenough, J.B. and Park, K.-S., *The Li-Ion Rechargeable Battery: A Perspective.* Journal of the American Chemical Society, 2013. **135**(4): p. 1167-1176.
2. Liu, P., Ross, R., and Newman, A., *Long-range, low-cost electric vehicles enabled by robust energy storage.* MRS Energy & Sustainability, 2015. **2**.
3. Lu, L., Han, X., Li, J., Hua, J., and Ouyang, M., *A review on the key issues for lithium-ion battery management in electric vehicles.* Journal of Power Sources, 2013. **226**: p. 272-288.
4. Waag, W., Fleischer, C., and Sauer, D.U., *Critical review of the methods for monitoring of lithium-ion batteries in electric and hybrid vehicles.* Journal of Power Sources, 2014. **258**: p. 321-339.
5. Giurgiutiu, V., *Structural health monitoring: with piezoelectric wafer active sensors*. 2007: Academic Press.
6. Sood, B., Osterman, M., and Pecht, M. *Health monitoring of lithium-ion batteries*. in *Product Compliance Engineering (ISPCE), 2013 IEEE Symposium on*. 2013. IEEE.
7. Gold, L., Bach, T., Virsik, W., Schmitt, A., Müller, J., Staab, T.E., and Sextl, G., *Probing lithium-ion batteries' state-of-charge using ultrasonic transmission–Concept and laboratory testing.* Journal of Power Sources, 2017. **343**: p. 536-544.

8. Hsieh, A., Bhadra, S., Hertzberg, B., Gjeltema, P., Goy, A., Fleischer, J., and Steingart, D., *Electrochemical-acoustic time of flight: in operando correlation of physical dynamics with battery charge and health.* Energy & environmental science, 2015. **8**(5): p. 1569-1577.
9. Ladpli, P., Kopsaftopoulos, F., Nardari, R., and Chang, F.-K., *Battery charge and health state monitoring via ultrasonic guided-wave-based methods using built-in piezoelectric transducers*, in *SPIE Smart Structures and Materials+ Nondestructive Evaluation and Health Monitoring*. 2017, International Society for Optics and Photonics. p. 1017108-1017108-12.
10. Ladpli, P., Nardari, R., Kopsaftopoulos, F., Wang, Y., and Chang, F.-K., *Design of Multifunctional Structural Batteries with Health Monitoring Capabilities*, in *European Workshop on Structural Health Monitoring 2016*. 2016: Bilbao, Spain.
11. Ladpli, P., Nardari, R., and Chang, F.-K., *Multifunctional Energy Storage Composites*. 2016: United States.
12. Ladpli, P., Nardari, R., Rewari, R., Liu, H., Slater, M., Kepler, K., Wang, Y., Kopsaftopoulos, F., and Chang, F.-K., *Multifunctional Energy Storage Composites: Design, Fabrication, and Experimental Characterization*, in *ASME 2016 Energy Storage Forum*. 2016, American Society of Mechanical Engineers: Charlotte, NC. p. V002T01A004-V002T01A004.
13. Ladpli, P., Nardari, R., Wang, Y., Hernandez-Gallegos, P.A., Rewari, R., Kuo, H.T., Kopsaftopoulos, F., Kepler, K.D., Lopez, H.A., and Chang, F.-K., *Multifunctional Energy Storage Composites for SHM Distributed Sensor Networks*, in *International Workshop on Structural Health Monitoring 2015*. 2015: Stanford, CA.
14. Pavlakovic, B. and Lowe, M., *Disperse user's manual version 2.0. 11.* Imperial College, Univ of London, 2001.
15. Pavlakovic, B., Lowe, M., Alleyne, D., and Cawley, P., *Disperse: a general purpose program for creating dispersion curves*, in *Review of progress in quantitative nondestructive evaluation*. 1997, Springer. p. 185-192.
16. Rieger, B., Erhard, S.V., Rumpf, K., and Jossen, A., *A new method to model the thickness change of a commercial pouch cell during discharge.* Journal of The Electrochemical Society, 2016. **163**(8): p. A1566-A1575.
17. Wu, L. and Zhang, J., *Ab initio study of anisotropic mechanical properties of LiCoO2 during lithium intercalation and deintercalation process.* Journal of Applied Physics, 2015. **118**(22): p. 225101.
18. Linden, D. *Handbook of batteries*. in *Fuel and Energy Abstracts*. 1995.
19. Qi, Y., Guo, H., Hector, L.G., and Timmons, A., *Threefold increase in the Young's modulus of graphite negative electrode during lithium intercalation.* Journal of The Electrochemical Society, 2010. **157**(5): p. A558-A566.
20. Hastie, T. and Tibshirani, R., *Generalized additive models*. 1990: Wiley Online Library.
21. Wood, S.N., *mgcv: GAMs and generalized ridge regression for R.* R news, 2001. **1**(2): p. 20-25.
22. Akaike, H., *Information theory and an extension of the maximum likelihood principle*, in *Selected Papers of Hirotugu Akaike*. 1998, Springer. p. 199-213.